THE JOURNAL OF BIOLOGICAL CHEMISTRY
Vol. 280, No. 26, Issue of July 1, pp. 25225–25232, 2005
Printed in U.S.A.

Cross-talk between fMLP and Vitronectin Receptors Triggered by Urokinase Receptor-derived *SRSRY* Peptide*

Received for publication, November 8, 2004, and in revised form, April 29, 2005
Published, JBC Papers in Press, May 2, 2005, DOI 10.1074/jbc.M412605200

Lucia Gargiulo‡§, Immacolata Longanesi-Cattani‡§, Katia Bifulco‡, Paola Franco¶, Rosanna Raiola‡, Pietro Campiglia‖, Paolo Grieco‖, Gianfranco Peluso‡, M. Patrizia Stoppelli¶, and Maria V. Carriero‡**

From the ‡Department of Experimental Oncology, National Cancer Institute, 80131 Naples, Italy, ¶Institute of Genetics and Biophysics, "Adriano Buzzati-Traverso," 80125 Naples, Italy, and ‖Department of Pharmaceutical Chemistry and Toxicology, University Federico II, 80131 Naples, Italy

The urokinase-type plasminogen activator receptor (uPAR) sustains cell migration through its capacity to promote pericellular proteolysis, regulate integrin function, and mediate chemotactic signaling in response to urokinase. We have characterized the early signaling events triggered by the Ser-Arg-Ser-Arg-Tyr (SRSRY) chemotactic uPAR sequence. Cell exposure to SRSRY peptide promotes directional migration on vitronectin-coated filters, regardless of uPAR expression, in a specific and dose-dependent manner, with maximal effect at a concentration level as low as 10 nM. A similar concentration profile is observed in a quantitative analysis of SRSRY-dependent cytoskeletal rearrangements, mostly consisting of filamentous structures localized in a single cell region. SRSRY analogues with alanine substitutions fail to drive F-actin formation and cell migration, indicating a critical role for each amino acid residue. As with ligand-dependent uPAR signaling, SRSRY stimulates protein kinase C activity and results in ERK1/2 phosphorylation. The involvement of the high affinity *N*-formyl-Met-Leu-Phe receptor (FPR) in this process is indicated by the finding that 100 nM *N*-formyl-Met-Leu-Phe inhibits binding of D2D3 to the cell surface, as well as SRSRY-stimulated cell migration and F-actin polarization. Moreover, cell exposure to SRSRY promotes FPR-dependent vitronectin release and increased uPAR·αvβ5 vitronectin receptor physical association, indicating that αvβ5 activity is regulated by the SRSRY uPAR sequence via FPR. Finally, we provide evidence that αvβ5 is required for SRSRY-dependent ERK1/2 phosphorylation, whereas it is not required for protein kinase C activation. The data indicate that the ability of uPAR to stimulate cell migration and cytoskeletal rearrangements is retained by the SRSRY peptide alone and that it is supported by cross-talk between FPR and αvβ5.

Cell migration is the result of a complex balance among localized proteolysis, dynamic cell/extracellular matrix interactions, and cytoskeletal organization. The receptor for the urokinase-type plasminogen activator (uPAR)[1] appears to be a key molecule in the coordination of these different events (1, 2). The uPAR promotes cell-associated proteolysis by binding to its specific ligand, the serine protease urokinase (uPA), which locally converts plasminogen into active plasmin, thus favoring tissue invasion by tumor cells and metastasis (3–5). In several cell lines, ligand-engaged uPAR stimulates migration by activating PKC, MEK, c-Raf, phosphatidylinositol 3-kinase, Rac, and pp125FAK (6–8). Despite the lack of a trans-membrane domain, the uPAR is able to activate intracellular signaling, possibly by interaction with other trans-membrane receptors. Indeed, there is abundant evidence that uPAR is associated in large molecular complexes with integrins, caveolin, and Src kinases (8–13). Direct binding of uPAR and integrins has been shown *in vitro* (11), and a peptide disrupting uPAR-integrin association also prevents uPAR signaling (14). The reversible association with other receptors is supported by the lateral mobility of uPAR in the plasma membrane bilayer and its redistribution upon interaction with uPA in focal adhesions (15). The uPAR itself is an adhesion receptor because it binds to vitronectin, an abundant component of extracellular matrix (16, 17). The interactions with integrins and vitronectin are positively regulated by uPA (17, 18), and both uPA and vitronectin can induce uPAR-mediated cytoskeletal reorganization and cell migration (8, 12, 19).

The uPAR is a member of the Ly6/α-neurotoxin/uPAR protein domain family (20). It consists of three domains connected by linker regions of 15–20 amino acids each (21). The N-terminal D1 domain interacts with uPA, and it is also required for binding to vitronectin, thus suggesting the cooperation of different domains (20). D2 connects D1 and the C-terminal D3 domain bearing a glycophosphatidylinositol anchor (21). Enzymatic cleavage of the glycophosphatidylinositol anchor results in a soluble form of the receptor, which has been detected in human plasma and urine (22, 23). The soluble uPAR, deprived of the D1 domain by cleavage with chymotrypsin or full-length uPA, is a potent chemoattractant for monocyte-like cells (24). In fact, enzymatic cleavage unmasks a region with chemotactic properties, corresponding to residues 88–92 of uPAR (P88-92) (24, 25).

* This work was supported by the Italian Association for Cancer Research, Ricerca Finalizzata Ministero della Salute 2003, and the European Union Framework Programme 6 (LSHC-CT-2003-503297). The costs of publication of this article were defrayed in part by the payment of page charges. This article must therefore be hereby marked "*advertisement*" in accordance with 18 U.S.C. Section 1734 solely to indicate this fact.

§ Both authors contributed equally to this work.

** To whom correspondence should be addressed: Dept. of Experimental Oncology, National Cancer Institute of Naples, Via M. Semmola, 80131 Naples, Italy. Tel.: 39-081-5903569; Fax: 39-081-5903814; E-mail: mariolina.carriero@fondazionepascale.it.

[1] The abbreviations used are: uPAR, urokinase-type plasminogen activator receptor; uPA, urokinase-type plasminogen activator; LM, laminin; CG, collagen; FN, fibronectin; VN, vitronectin; fMLP, *N*-formyl-Met-Leu-Phe; FPR, fMLP receptor; PKC, protein kinase C; ERK, extracellular signal-regulated kinase; mAb, monoclonal antibody; Ab, antibody; MEK, mitogen-activated protein kinase/extracellular signal-regulated kinase kinase; HPLC, high pressure liquid chromatography; PBS, phosphate-buffered saline; PTX, pertussis toxin.

The synthetic peptide Ser-Arg-Ser-Arg-Tyr (SRSRYp) carrying this epitope has been reported to be chemotactically active (24). Resnati *et al.* (26) have recently reported that P88-92-induced chemotaxis is mediated by the low affinity receptor for *N*-formyl-Met-Leu-Phe (fMLP), a bacterial chemotactic peptide. Accordingly, the $D2D3_{88-274}$ uPAR fragment was identified as an endogenous ligand for FPRL1/LXA4R that is necessary and sufficient to mediate $D2D3_{88-274}$-dependent chemotaxis (26). Whereas uPA-dependent cell migration requires the expression of intact uPAR including D1, fMLP-dependent cell migration requires the expression of P88-92 containing uPAR and is uPA- and D1-independent (27).

To investigate the early events as well as the partners involved in the complex membrane interactions characterizing uPAR activation, we have simplified our analysis, focusing on the signaling effects of SRSRYp. We now provide evidence that SRSRYp triggers cross-talk between high affinity fMLP (FPR) and αvβ5 vitronectin receptors, resulting in cytoskeletal rearrangements and cell migration.

EXPERIMENTAL PROCEDURES

Reagents—Recombinant D1 (residues 1–87), D2 (residues 88–183), D3 (residues 184–284), and D2D3 (residues 88–284) uPAR domains and the pertussis toxin (PTX) were from Calbiochem. Rhodamine-conjugated phalloidin, RGD peptide, fMLP, calphostin C, wortmannin, LY294002, and PD98059 were from Sigma. Native human vitronectin (VN), collagen IV (CG), fibronectin (FN), and laminin (LM) were purchased from Promega. Mouse anti-ERK1 and mouse anti-ERK2 monoclonal antibodies (mAbs) and rabbit anti-phospho-ERK1/2 antibodies (Abs) were from Santa Cruz Biotechnology. VNR147 anti-αv and P1F6 anti-αvβ5 mAbs and rabbit polyclonal anti-α1, anti-α2, anti-α3 anti-α5, and anti-αv Abs were from Chemicon International Inc. Anti-uPAR R4 mAb was a gift of Dr. Gunilla Hoyer-Hansen (Finsen Institute, Copenhagen, Denmark). The horseradish peroxidase-conjugated immunoglobulins, the enhanced chemiluminescence detection system (ECL), and the protein kinase C enzyme kit assay were from Amersham Biosciences. The tissue culture dishes, polycarbonate chemotaxis filters, and Boyden chambers were from Nucleopore. All cell culture reagents were purchased from Invitrogen.

Peptide Synthesis and Purification—Peptides were synthesized by the solid phase approach using standard Fmoc (*N*-(9-fluorenyl)methoxycarbonyl) methodology in a manual reaction vessel (28). The purification was achieved using a semi-preparative reversed-phase HPLC C18 bonded silica column (Vydac 218TP1010). The purified peptides were 99% pure as determined by analytical reversed-phase HPLC. The correct molecular weights were confirmed by mass spectrometry and amino acid analysis. Peptide stability was assessed by incubating each peptide with chymotrypsin for 4 h at 37 °C and subsequently analyzing the products by reversed-phase HPLC. Peptides exhibiting enzymatic digestion of <15% were employed in the assays.

Cell Cultures and Treatments—Human kidney embryonic 293 cells were grown in Dulbecco's modified Eagle's medium supplemented with 10% fetal calf serum, 100 IU/ml penicillin, and 50 μg/ml streptomycin. 293/uPAR cells were stably transfected with the human uPAR cDNA as described by Montuori *et al.* (27). Subconfluent 293 and 293/uPAR cells were detached by mild trypsinization, incubated with 10% fetal calf serum-Dulbecco's modified Eagle's medium for 1 h at 37 °C in 5% CO_2, briefly acid-treated to avoid any interference by serum-derived membrane-bound growth factors as previously described (18), washed with PBS, and counted. In some experiments, the cells were pre-incubated for 1 h at 37 °C with 200 nM calphostin C, 25 μM PD98059, 1 μM wortmannin, or 20 μM LY294002, or they were cultured for 18 h at 37 °C with 50 ng/ml PTX. Desensitization was carried out by pre-incubating cells with 100 nM fMLP for 30 min at 37 °C in 5% CO_2 as described previously (26). When indicated, RGD peptide (50 μg/ml) or the indicated Abs (5 μg/ml) were pre-incubated with the cell suspension for 1 h at room temperature and kept throughout the assay.

Cell Migration—Subconfluent 293 and 293/uPAR cells were detached, briefly acid-treated to avoid any interference by serum-derived membrane-bound growth factors, and subjected to cell migration assays using conventional Boyden chambers (8). Migration toward the indicated chemoattractants, which were diluted in serum-free Dulbecco's modified Eagle's medium, was performed for 4 h using filters (pore size, 8-μm) coated with 5 μg/ml VN, unless otherwise specified. The random cell migration was considered as 100%, and directional cell migration was calculated as a percentage of the random cell migration.

Analysis of Cytoskeleton—Detached and acid-treated subconfluent 293 and 293/uPAR cells were analyzed for their cytoskeletal organization upon exposure to the indicated peptides or isolated uPAR domains for 1 h at 23 °C, unless otherwise specified. Cell pellets were washed with PBS, fixed with 2.5% formaldehyde, permeabilized with 0.1% Triton X-100 for 10 min at 4 °C, and then incubated with 0.1 μg/ml rhodamine-conjugated phalloidin for 40 min (8). After extensive washing with PBS, cells were placed on a clean glass slide and examined either by a fluorescence inverted microscope or by a confocal microscope (Leica). A total of 200 cells/sample were examined; cells exhibiting rhodamine-phalloidin-positive protrusions were counted and expressed as a percentage of total estimated cells. The percentages of cells exhibiting F-actin single polarizations upon exposure to effectors were subtracted of the percentage of cells exhibiting phalloidin protrusions in the absence of treatment.

Binding Assay—5 μg of D2D3 were radio-iodinated with $Na^{125}I$ using IODO-GEN as previously described (29). The radiolabeled protein was purified from unbound iodide by Sephadex G-25 chromatography, and the resulting specific activity was ~30 μCi/μg. 293 cells (1×10^6 cells/sample) were incubated with ^{125}I-D2D3 (1 nM) in binding medium (Dulbecco's modified Eagle's medium containing 1 mg/ml bovine serum albumin and 25 mM Hepes, pH 7.5) at 4 °C for 60 min, in the presence or in the absence of an increasing concentration of unlabeled D2D3 or other competitors. After extensive washing, cell-associated radioactivity was assessed in a gamma counter. Binding in the presence of 1 μM unlabeled D2D3 was subtracted to obtain the specific binding. The extent of inhibition was calculated relative to the specific binding, which was taken as 100%.

Cell Adhesion—24-well flat-bottom dishes were incubated with a PBS solution containing 2.5 μg/ml LM, CG, FN, VN, or heat-denatured bovine serum albumin (−) overnight at 4 °C. Other experiments were performed using plates coated with 2.5 μg/ml D1, D2, or D3 recombinant uPAR domains. In all cases, plates were rinsed with PBS, incubated for 1 h at 23 °C with 1% heat-denatured bovine serum albumin, and rinsed again. Desensitized or untreated cells (1.5×10^5 cells/well) were seeded for 2 h at 37 °C in 5% CO_2, in the presence or absence of 10 nM SRSRYp. When indicated, cells were pre-incubated with 5 μg/ml anti-αvβ5 mAb or diluents for 1 h at 23 °C. Adherent cells were detached by trypsinization and counted.

Protein Kinase C Enzyme Assay—293 cells (5×10^4 cells/sample) were detached by a mild trypsinization, exposed to 10 nM SRSRYp for 5 or 10 min at 23 °C, and then lysed in 50 μl of 50 mM Tris/HCl, pH 7.5, 0.3% (w/v) β-mercaptoethanol, 5 mM EDTA, 10 mM EGTA, 50 μg/ml phenylmethylsulfonyl fluoride, and 10 mM benzamidine. PKC activity was assessed for 15 min at 37 °C in the presence of 0.2 μCi/sample [γ-^{32}P]ATP by a PKC kit assay (Amersham Biosciences) according to the manufacturer's instructions. Nonspecific adsorption of [^{32}P]ATP to filter paper was determined by omitting cell lysate (blank). The extent of PKC-dependent phosphorylation is expressed as pmol phosphate transferred/min.

Western Blot—Cell lysates were prepared with radioimmune precipitation assay buffer (140 mM NaCl, 10 mM Tris/HCl, pH 7.5, 0.1% SDS, 1% Triton X-100, 1 mM Na_2VO_4, and protease inhibitor mixture) and cleared by centrifugation. 50 μg of proteins per sample were separated on a 10% SDS-PAGE and transferred to a nitrocellulose membrane. Membranes were blocked with 5% nonfat dry milk and probed with 2 μg/ml anti-phospho-ERK1/2, anti-α1, anti-α2, anti-α3, anti-α5, or anti-αv polyclonal Abs. Filters were then incubated with horseradish peroxidase-conjugated anti-rabbit Abs for 1 h at 23 °C and detected by ECL. Total ERK1/2 was quantitated by reprobing filters with 2 μg/ml anti-ERK1 and anti-ERK2 mAbs. Densitometry of autoradiographic bands was analyzed using National Institutes of Health (Bethesda, MD) Image 1.62 software.

Co-immunoprecipitation—For the analysis of uPAR·αv complexes, detached and acid-treated 293/uPAR cells were exposed to 100 nM fMLP or diluents at 37 °C in 5% CO_2 for 30 min and then incubated with SRSRYp or diluents for 1 h. Following the indicated treatments, cells were lysed in radioimmune precipitation assay buffer and cleared by centrifugation at 12,000 rpm, and 400 μg/sample were incubated overnight at 4 °C with 5 μg/ml VNR147 anti-αv mAb. The immunoprecipitated proteins recovered by absorption to protein G-Sepharose and separated onto a 10% SDS-PAGE under nonreducing conditions were transferred to nitrocellulose membranes. Western blots were performed by incubating filters with 2 μg/ml R4 anti-uPAR mAb or anti-αv polyclonal Ab for 2 h at 4 °C.

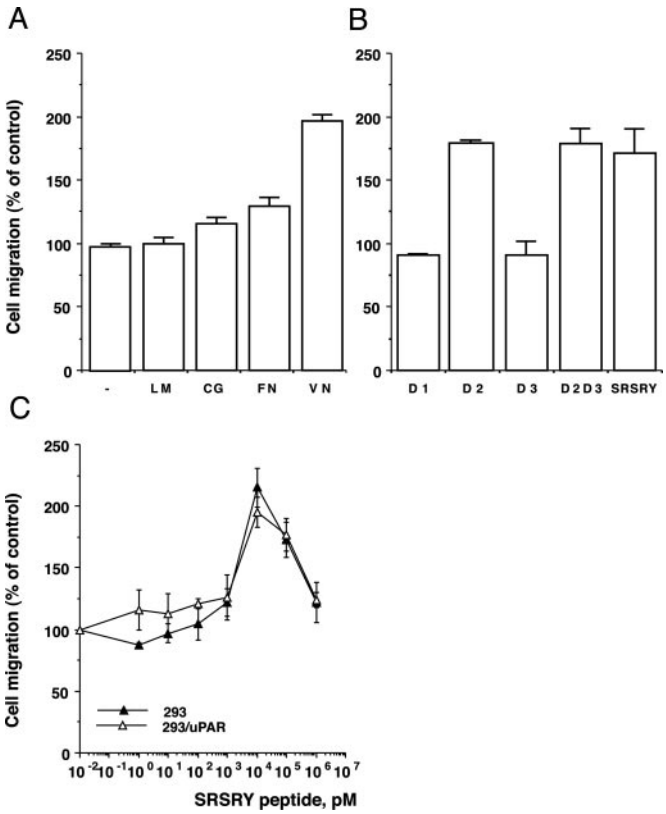

FIG. 1. **Effect of the chemotactic uPAR sequence on directional cell migration.** *A*, chemotactic response of 293 cells to 10 nM SRSRYp in a Boyden chamber assay, using uncoated filters (−) or filters coated with LM, CG, FN, or VN. *B*, chemotactic response of 293 cells to 10 nM of the indicated uPAR domains or SRSRYp on VN-coated filters. *C*, chemotactic response of 293 and 293/uPAR cells to the indicated picomolar concentrations of SRSRYp on VN-coated filters. Random cell migration was considered as 100%, and directional cell migration was calculated as a percentage of the random cell migration. The data represent the average of three experiments, all performed in triplicate, with S.E. indicated by *error bars*.

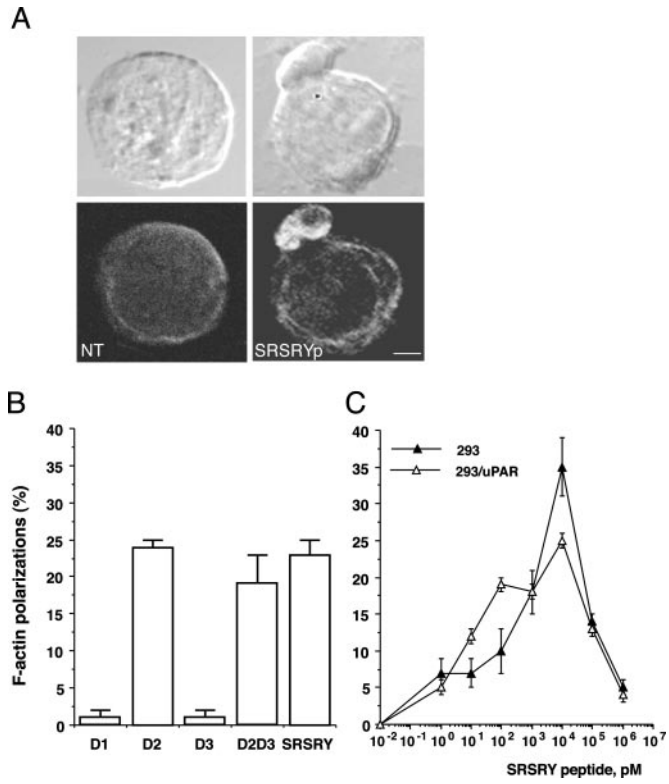

FIG. 2. **Effect of SRSRY peptide on cell cytoskeletal organization.** *A*, 293 cells were incubated with diluents (*NT*) or 10 nM SRSRYp for 1 h at 23 °C and subsequently stained with rhodamine-phalloidin. Representative cells for each condition are shown. *Bar*, 5 μm. *B*, histogram values correspond to the net percentage of 293 cells exhibiting F-actin single polarizations upon exposure to the indicated effectors (10 nM). *C*, net percentage of 293 and 293/uPAR cells exhibiting F-actin single polarizations upon exposure to the indicated picomolar concentrations of SRSRYp. Data are the average of three experiments performed in triplicate and evaluated by two independent observers, with S.E. indicated by *error bars*.

RESULTS

Effect of the SRSRY Sequence and Isolated uPAR Domains on Cell Migration and Cytoskeleton—Within uPAR, the SRSRY sequence (residues 88–92) has been identified as having potent chemotactic activity in a number of cell lines, including murine $uPAR^{-/-}$ fibroblasts (24). In an effort to dissect the molecular events underlying uPAR signaling, we first determined the optimal conditions supporting chemotaxis toward synthetic SRSRYp. In a conventional Boyden chamber assay, we tested the ability of SRSRYp to promote cell migration of human embryonic kidney 293 cells on uncoated filters or filters coated with LM, CG, FN, or VN: the 293 cell line was selected because it has no detectable uPARs (27). As shown in Fig. 1*A*, 10 nM SRSRYp did not promote appreciable chemotaxis of 293 cells on uncoated or LM-coated filters, whereas a slight increase in migration was detected on CG- or FN-coated filters. On the other hand, on VN-coated filters, SRSRYp and isolated uPAR domains (D2 or D2D3) containing residues 88–92 consistently increased directional cell migration to a similar extent (Fig. 1, *A* and *B*). As expected, portions of the D1 and D3 domains that did not include residues 88–92 were ineffective (Fig. 1*B*). SRSRYp motogen activity exerted on VN-coated surfaces is dose-dependent, with maximal induction being obtained at about 10 nM. Interestingly, this chemotactic effect is uPAR-independent because it occurs in both uPAR-lacking and uPAR-bearing 293 cells (Fig. 1*C*). In order to investigate the early intracellular effects of the chemotactic SRSRY sequence, we analyzed the cytoskeletal organization of pre-adherent 293 cells and of 293/uPAR cells exposed to SRSRYp for 60 min at 23 °C. As the confocal images show, exposure to 10 nM SRSRYp strongly modified the distribution of F-actin, with the appearance of peripheral filamentous structures, resembling those observed in uPAR-bearing cell lines exposed to uPA, often localized at one pole of the cell. Light microscopy images show that rhodamine-phalloidin staining corresponds to lamellipodia-like protrusions (Fig. 2*A*). A similar pattern was observed when incubation was performed at 37 °C (data not shown). To extract quantitative data from these experiments, a total of 200 cells/sample were examined, and the percentage of cells exhibiting phalloidin-positive protrusions was determined. The percentage of cells exhibiting F-actin single polarization in the absence of treatment (5 ± 1%) was subtracted to obtain net effector-dependent values. A net increase in F-actin-enriched regions following exposure to D2, D2D3 uPAR domains, or SRSRYp was observed in at least 20% of the total cell population (Fig. 2*B*). 10 nM D2 and 10 nM D2D3 uPAR domains promoted similar cytoskeletal rearrangements, whereas D1 or D3 produced no effect. SRSRYp caused clear-cut F-actin formation, which was again uPAR-independent and dose-dependent (Fig. 2*C*).

In order to pinpoint the functional importance of each individual amino acid in the chemotactic peptide, the I, II, III, IV, or I and III amino acid residues were substituted with alanine residues. The resulting peptides were first checked for cytotoxicity by a trypan blue assay. Then, they were tested for their ability to promote migration and cytoskeletal rearrangements

TABLE I
Effects of SRSRY-derived Ala-substituted peptides on cell migration and cytoskeletal organization

Cell migration toward the indicated peptides is assessed as described under "Experimental Procedures." For analysis of F-actin polymerization, a total of 200 cells/sample were examined, and cells exhibiting phalloidin-positive protrusions were expressed as a percentage of total cell number. The percentage of cells exhibiting F-actin single polarizations in the absence of treatment was subtracted to obtain the net effector-dependent values. Data points are the mean ± S.E. mean of three independent experiments.

Effectors (10 nM)	Cell migration (%)		F-actin polarizations (%)	
	293 cells	293/uPAR cells	293 cells	293/uPAR cells
SRSRY	233 ± 7	208 ± 6	22 ± 1	21 + 2
ARSRY	122 ± 5	100 ± 5	4 ± 3	2 ± 1
SASRY	107 ± 1	101 ± 4	3 ± 3	5 ± 4
SRARY	104 ± 1	102 ± 5	3 ± 2	4 ± 3
SRSAY	101 ± 6	104 ± 2	1 ± 0	2 ± 2
ARARY	104 ± 5	105 ± 12	1 ± 1	1 ± 1

of 293 and 293/uPAR cells. All modified peptides failed to increase cell motility and F-actin polarizations, showing that all five amino acids in the peptide are critical to these functions (Table I). The clear-cut biological activity of the wild type chemotactic peptide, together with the lack of activity of all Ala-substituted peptides, strongly supports an important role for the SRSRY sequence in uPAR-dependent signaling.

Effect of Signaling Inhibitors on SRSRY-dependent Cytoskeletal Reorganization and Cell Migration—Increasing evidence supports the notion that uPAR-mediated signaling involves a number of signal transducers, including G proteins, PKC, phosphatidylinositol 3-kinase, and mitogen-activated protein kinases (6, 8, 13, 30). Others have shown that a G protein-coupled receptor is required for SRSRY-dependent chemotaxis (24). We have previously reported that uPAR engagement by uPA triggers F-actin polymerization in pre-adherent cells (8). To assess whether the wild type SRSRY sequence and ligand-activated full-length uPAR share the same downstream mediators, 293/uPAR cells were pre-treated with specific signaling inhibitors and then exposed to SRSRYp, recombinant bacterial uPA, or diluents prior to rhodamine-phalloidin staining. Both SRSRYp and uPA fail to induce cytoskeletal rearrangements in the presence of PTX, calphostin C, or PD98059, showing the involvement of a G protein-coupled receptor, PKC, and MEK1 activities (Table II). Accordingly, phosphorylation of ERK1/2 in 293 cells exposed to 10 nM SRSRYp for 5, 10, 20, and 30 min was increased by 2–3-fold within 5–10 min (Fig. 3*A*). The effect is dose-dependent, with an optimum concentration at 0.1 nM (Fig. 3*B*). Moreover, pre-treatment of cells with wortmannin or LY294002, both of which are inhibitors of phosphatidylinositol 3-kinase, blocked uPA-dependent effects and substantially reduced SRSRY-dependent effects on the cytoskeleton. These molecules also prevented SRSRY-dependent cytoskeletal rearrangements in the absence of uPAR. Remarkably, in 293/uPAR cells, all were effective in inhibiting SRSRY-dependent cell migration (Table II). Overall, these results show that SRSRYp impinges on cell cytoskeleton and directs migration in a manner similar to that of the uPA·uPAR complex, indicating that SRSRY- and uPA·uPAR-dependent signaling share several common mediators that have intricate relationships.

Requirement of αvβ5 in FPR High Affinity fMLP Receptor-mediated and SRSRY-dependent Signaling—The $D2D3_{88-274}$ uPAR fragment has been identified as an endogenous ligand for FPRL1/LXA4R low affinity fMLP receptor, a G protein-coupled receptor (26). More recently, we have found that 293 cells, which do not express a detectable amount of uPAR and FPRL1/LXA4R low affinity fMLP receptor, do express significant levels of FPR high affinity fMLP receptor (27). A competition assay showed saturable binding of an iodinated D2D3 uPAR fragment to the surface of 293 cells, with an apparent K_d of about 30 nM (data not shown). Binding was competed by excess unlabeled D2D3 or SRSRYp, but not by peptides containing alanine substitutions (Table III). Because binding of iodinated D2D3 to 293 cells is abrogated by pre-treatment with 100 nM fMLP (which is sufficient to desensitize FPR but not FPRL1; Table III), we tested the possibility that FPR may act as a mediator of SRSRY biological activity. To this end, 293 and 293/uPAR cells were desensitized with 100 nM fMLP and then tested for their ability to migrate toward fMLP or SRSRYp. The number of untreated cells counted on the lower filter surface in the absence of chemoattractant was comparable to that of desensitized cells (49 ± 7 and 54 ± 6, respectively). As previously reported by Montuori *et al.* (27), fMLP failed to promote migration of 293 cells. Whereas untreated 293 cells migrate toward SRSRYp, desensitized 293 cells do not migrate in response to an increasing concentration of fMLP or 10 nM SRSRYp (Fig. 4, *A* and *B*). As expected, 293/uPAR cells previously subjected to desensitization lose the ability to migrate toward fMLP or SRSRYp (Fig. 4, *A* and *B*). Although chemotaxis toward serum is slightly reduced by desensitization, a clear-cut and specific inhibition of fMLP- and SRSRY-dependent migration is observed in desensitized 293/uPAR cells (Fig. 4*B*). In agreement with the cell migration experimental results, the incubation of desensitized 293 cells with 10 nM SRSRYp did not produce F-actin single polarizations (data not shown). Overall, these results indicate that the SRSRY-triggered signaling is directly mediated by the FPR receptor.

We have previously demonstrated that uPA-dependent F-actin polymerization and cell migration require the uPAR as well as the αvβ5 vitronectin receptor (8). Others have shown the involvement of several integrin-type receptors in uPAR-dependent signaling (11). Because 293 cells do express α1, α3, α5, and αv integrin α chains (Fig. 4*C*, *inset*), we considered the possibility that SRSRY-dependent signaling may be mediated by any of these integrins. Therefore, SRSRY-dependent 293 cell motility was analyzed in the presence of RGD peptide, anti-α1 Ab, anti-α3 Ab, anti-α5 Ab, anti-αv Ab, P1F6 anti-αvβ5 blocking mAb, or nonimmune serum. Whereas nonimmune serum, anti-α1 Ab, or anti-α3 Ab failed to inhibit SRSRY-dependent cell migration, a slight decrease was exerted by anti-α5 Ab (Fig. 4*C*). On the other hand, SRSRY-induced 293 directional cell migration is αvβ5-mediated because it is prevented by pre-incubating cells with anti-αvβ5 mAb, anti-αv Ab, or RGD peptide (Fig. 4*C*). Indeed, pre-exposure of 293 or 293/uPAR cells to anti-αvβ5 mAb, anti-αv Ab, or RGD peptide prevented SRSRY-induced single F-actin polarizations (Fig. 4*D*). These findings, taken together, suggest that SRSRY-induced and FPR-mediated signaling requires αvβ5 integrin.

Cross-talk between FPR and αvβ5 Receptors Triggered by the SRSRY Peptide—The involvement of αvβ5 integrin is in keeping with the increased SRSRY-dependent migration on VN-coated surfaces shown in Fig. 1*A*. To investigate whether the SRSRY sequence plays a role in integrin activation, we tested whether SRSRYp may affect αvβ5 vitronectin receptor avidity and modify the adhesion of 293 cells onto extracellular matrix proteins. The addition of 10 nM SRSRYp strongly decreases 293 cell adhesion onto VN, whereas no effect was observed on adhesion to LM-, CG-, or FN-coated dishes (Fig. 5*A*). Because the SRSRY-dependent decrease in cell adhesion to VN was abrogated by cell desensitization with 100 nM fMLP (Fig. 5*A*), we suggest that the SRSRY sequence interacts with FPR, which in turn specifically affects αvβ5·VN interaction, causing vitronectin release. As shown in Table II, specific signaling inhibitors prevent ERK1/2 phosphorylation and PKC activa-

TABLE II
Effect of signaling inhibitors on SRSRY-dependent cytoskeletal organization and cell migration

Cells were pre-incubated with calphostin C, wortmannin, LY294002, or PD98059 inhibitors for 1 h at 37 °C or cultured with PTX for 18 h at 37 °C. For analysis of F-actin polymerization, cells were treated with recombinant uPA or SRSRYp, and the percentage of cells exhibiting F-actin single polarizations was assessed as described in the legend to Table I. Cell migration toward uPA or SRSRYp was assessed as described under "Experimental Procedures." Data points are the mean ± S.E. of three independent experiments.

Pre-treatment	F-actin polarizations (%)			Cell migration (%)	
	293-/uPAR cells		293cells	293-/uPAR cells	
	1 nM uPA	10 nM SRSRYp	10 nM SRSRYp	1 nM uPA	10 nM SRSRYp
Control	26 ± 3	21 ± 3	21 ± 3	253 ± 8	199 ± 5
PTX (50 ng/ml)	1 ± 1	1 ± 1	1 ± 1	102 ± 2	100 ± 2
Calphostin C (200 nM)	1 ± 1	1 ± 1	1 ± 1	97 ± 3	91 ± 14
Wortmannin (1 μM)	2 ± 0	5 ± 1	6 ± 1	104 ± 1	102 ± 6
LY294002 (20 μM)	1 ± 2	7 ± 1	6 ± 1	111 ± 4	101 ± 3
PD98059 (25 μM)	1 ± 1	1 ± 1	1 ± 1	94 ± 5	95 ± 10

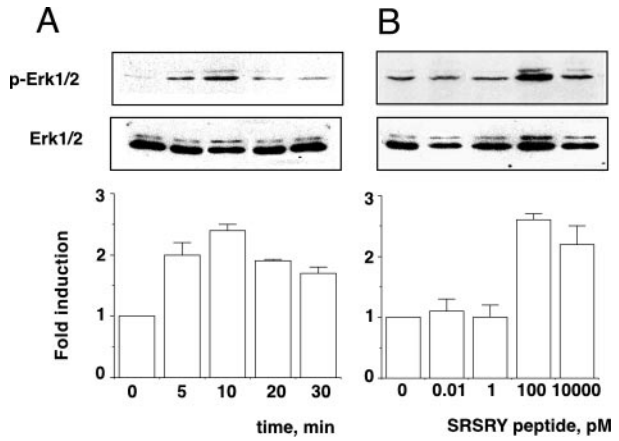

FIG. 3. **Effect of SRSRY peptide on ERK1/2 activation.** 293 cells were treated with 10 nM SRSRYp for the indicated times (*A*) or with the specified concentrations of SRSRYp for 10 min (*B*). ERK1/2 detection and quantitation were performed as specified under "Experimental Procedures." Data are means of two experiments, with S.E. indicated by *error bars*.

TABLE III
Binding specificity of iodinated D2D3 on 293 cells

Cells were incubated with ^{125}I-D2D3 at 4 °C for 60 min in the presence or absence of the indicated competitors. Cell-associated radioactivity obtained in the presence of 1 μM unlabeled D2D3 was subtracted to obtain the specific binding. The extent of inhibition by competitors was calculated relative to the specific binding, which was taken as 100%. Results were expressed as a mean of values obtained for three experiments, each performed on triplicate samples.

Unlabeled competitor	% Competition
D2D3 (1 μM)	100
SRSRY (10 μM)	43 ± 3
ARSRY (10 μM)	2 ± 2
SASRY (10 μM)	8 ± 5
SRARY (10 μM)	14 ± 1
SRSAY (10 μM)	3 ± 2
ARARY (10 μM)	1 ± 1
fMLP (100 nM)	100 ± 9

tion in cells exposed to SRSRYp. To investigate the role of FPR and αvβ5 vitronectin receptor in these mechanisms, ERK1/2 and PKC activities were analyzed in 293 cells desensitized with fMLP or pre-incubated with anti-αvβ5 or anti-αv Ab. As shown in Fig. 5*B*, SRSRYp loses the ability to elicit ERK1/2 phosphorylation in desensitized 293 cells, indicating that FPR is a mediator of ERK1/2 activation. Also, pre-incubation with anti-αvβ5 mAb or anti-αv Abs abrogates SRSRY-dependent ERK1/2 phosphorylation, indicating that αvβ5 is required for ERK1/2 activation (Fig. 5*B*). To further investigate the early events of SRSRY signaling, PKC activity was estimated in 293 cells exposed to SRSRYp. Exposure of 293 cells to 10 nM SRSRYp produced a time-dependent increase in the activity of PKC, peaking at 5 min (Table IV). Interestingly, SRSRY-dependent PKC activation is retained in the presence of anti-αvβ5 and anti-αv Abs, whereas it is prevented by desensitization. These results are in agreement with the central role of FPR in SRSRY signaling because cell desensitization abrogates both PKC and ERK activation. They also provide evidence that αvβ5 is exclusively involved in SRSRY-triggered ERK1/2 phosphorylation and not in PKC activation.

In previous work on several cell lines, we observed an increase in physical association of uPAR to αvβ5 following exposure to uPA (8). More recently, we have shown that the D1 domain is required for efficient uPAR·αv association (27). However, integrin-mediated cell adhesion to plastic-immobilized uPAR domains, mimicking uPAR·integrin interaction, has been described, indicating the presence of different integrin binding sites in the uPAR (31). Therefore, we tested the possibility that SRSRYp may regulate the avidity of αvβ5 for uPAR domains. As a result, 293 cells exhibit a slight ability to adhere onto D1, D2, and D3 uPAR domains. The addition of 10 nM SRSRYp strongly increases the adhesion of 293 cells onto the D2 uPAR domain: this effect is prevented by pre-incubation with anti-αvβ5 mAb or by desensitization with fMLP (Fig. 5*C*). As expected, no effect was observed on D1 or D3 uPAR-coated dishes. These findings suggest that FPR, activated by SRSRYp, decreases VN·αvβ5 binding and increases uPAR·αvβ5 affinity. We have previously found that the SRSRY uPAR sequence is not directly involved in the uPAR·αvβ5 interaction (27). To assess whether the chemotactic sequence contributes to the uPAR·αvβ5 association, the extent of uPAR co-purifying with αv was quantitated following 293/uPAR cell exposure to SRSRYp for 1 h at 23 °C. Pre-incubation of intact cells with 10 or 100 nM SRSRYp strongly increases the amount of uPAR co-purified with αv chain, indicating that SRSRYp positively modulates the physical association between uPAR and αvβ5 (Fig. 5*D*). The involvement of the fMLP receptor in the uPAR·αvβ5 association is further supported by the finding that SRSRYp fails to increase uPAR·αvβ5 association in fMLP-desensitized 293/uPAR cells (Fig. 5*D*). Although we cannot exclude the involvement of other mediators, the data indicate a complex cross-talk between FPR and αvβ5 receptors, which are both indispensable for SRSRY-induced signaling.

DISCUSSION

This study sheds light on the early molecular events in uPAR signaling involving complex functional relationships among uPAR, G protein-coupled receptors, and integrins. We have investigated this process by taking advantage of a peptide corresponding to the SRSRY chemotactic sequence localized in the D1-D2 uPAR linker region. The data point to the conclusion that the ability of uPAR to stimulate cell migration and cytoskeletal rearrangements is mediated by cross-talk between

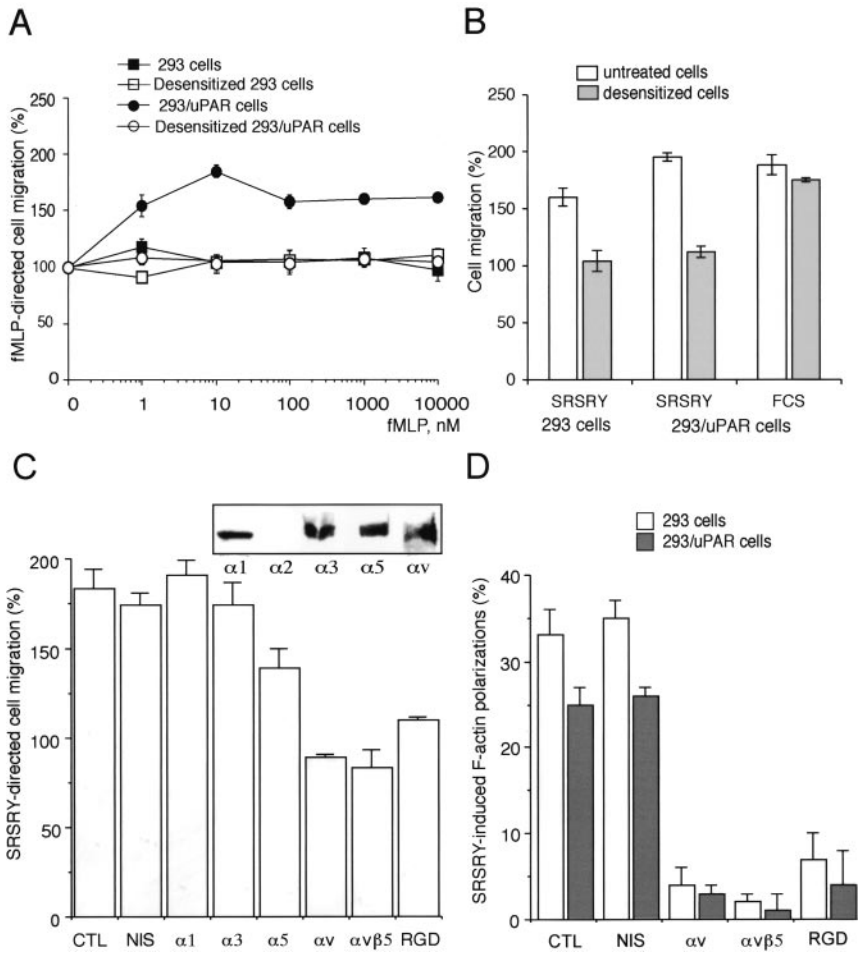

FIG. 4. **Requirement of FPR high affinity fMLP and αvβ5 vitronectin receptors in SRSRY-dependent signaling.** *A–C*, cell migration assays in Boyden chambers on VN-coated filters. Random cell migration was considered as 100%, and directional cell migration was calculated as a percentage of the random cell migration. Data points are the mean ± S.E. of three experiments. *A* and *B*, 293 and 293/uPAR cells were desensitized with 100 nM fMLP or diluents for 30 min at 37 °C and then subjected to chemotaxis to the indicated nanomolar concentrations of fMLP (*A*), 10 nM SRSRYp, or 10% fetal calf serum (*B*). *C*, 293 cells were pre-incubated without (*CTL*) or with 10% nonimmune serum (*NIS*), with 50 μg/ml RGD peptide, or with 5 μg/ml of the indicated antibodies and subjected to chemotaxis toward 10 nM SRSRYp. *Inset*, Western blot analysis of 293 total cell extracts (50 μg/sample) with anti-α1, -α2, -α3, -α5, or -αv integrin Ab. *D*, 293 and 293/uPAR cells were pre-incubated without (*CTL*), or with nonimmune serum (*NIS*), with 50 μg/ml RGD peptide, or with 5 μg/ml of the indicated antibody, exposed to 10 nM SRSRYp, and subsequently stained with rhodamine-phalloidin. Histogram values correspond to the net percentage of cells exhibiting F-actin single polarizations upon SRSRYp exposure. Data are the average of three experiments performed in triplicate, with S.E. indicated by *error bars*.

fMLP and αvβ5 vitronectin receptors. Evidence is provided that SRSRYp has major effects on actin polymerization, membrane protrusive activity, and motility of 293 embryonic kidney cells. SRSRY-dependent signaling is uPAR-independent, requires PKC and MEK activity, and results in ERK1/2 phosphorylation. Moreover, we provide evidence that high affinity fMLP and αvβ5 vitronectin receptors are both indispensable to SRSRY-induced signaling.

During this study, we found that inhibition of pathways previously reported to be involved in uPA-induced morphology changes and cell motility (*e.g.* activation of PTX-sensitive G proteins, PKC, ERK, or phosphatidylinositol 3-kinase) (7, 8, 12, 30) also prevents SRSRY-induced cytoskeletal changes. Although we cannot exclude the occurrence of additional mechanisms involving other regions of uPAR and uPA molecules, the data presented here fit well with the current notion that the signaling properties of uPAR are retained by the SRSRY sequence. Binding of SRSRY sequence to the seven-membrane-spanning domain FPRL1/LXA4R receptor for fMLP has been previously reported (26), and we have recently reported that uPAR chemotactic sequence induces motility via the high affinity FPR (27). Now we provide evidence for specific binding of the uPAR SRSRY sequence to FPR. The FPR activates a broad spectrum of fMLP-dependent cellular signaling events, including changes in cytoskeleton, motility, and PKC activity (32–34). In this study, we show that 293 cells migrate and reorganize their cytoskeleton upon exposure to SRSRYp, with the effects being prevented by cell desensitization with 100 nM fMLP. These data show not only that FPR is a mediator of uPAR signaling but also that SRSRY-triggered signaling requires changes in αvβ5 function. In a previous study, we showed that αvβ5-dependent signaling triggered by vitronectin did not require PKC, whereas uPAR-dependent signaling via αvβ5 did require PKC (8). Both findings suggest that uPAR is a cellular activator of several receptors, changing their function by orchestrating the formation of novel signaling complexes.

Interestingly, although 293 cells express all four of the α1, α3, α5, and αv integrin chains discretely, only anti-αv and anti-αvβ5 antibodies exert profound inhibitory effects on SRSRY-directed cell migration, from which we infer that, at least in 293 cells, the αvβ5 vitronectin receptor is involved. Several reports show the association of uPAR with αv (8, 12, 35). We have previously shown that the lateral interaction of uPAR with αv requires an intact receptor because removal of the D1 uPAR domain, regardless of the presence of the D1-D2 linker region that contains the chemotactic sequence, abolishes the lateral interaction of uPAR with integrins (27). The important role of αvβ5 in mediating SRSRY-dependent signaling is indicated by several lines of evidence: (*a*) the SRSRYp motogen effect occurs on vitronectin-coated filters, but not on filters that are uncoated or coated with collagen, laminin, or fibronectin; (*b*) anti-αvβ5 antibodies block SRSRY-dependent migration and cytoskeletal rearrangements; (*c*) exposure to SRSRYp inhibits cell adhesion to vitronectin; and (*d*) treatment of cells with SRSRYp results in increased physical association between uPAR and αvβ5. It is widely recognized that integrins are important functional partners for uPAR on the cell surface. Recent studies point to important structural features of uPAR association with integrins, revealing *in vivo* the occurrence of altered integrin function when uPAR-integrin interactions are impaired (11, 14, 36). Although a number of studies document the requirement of intact uPAR for an efficient binding to

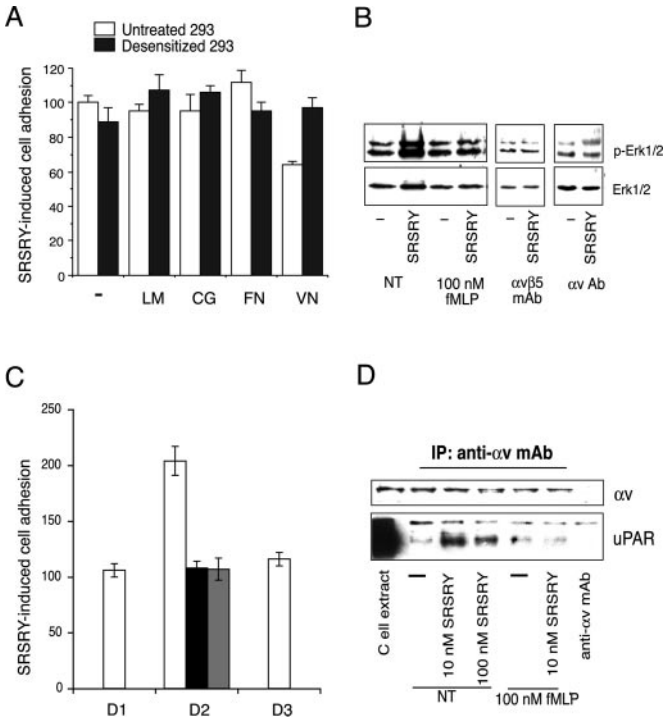

FIG. 5. **Cross-talk between fMLP and αvβ5 receptors triggered by the SRSRY peptide.** *A*, adhesion assays of 293 on LM, CG, FN, VN, or heat-denatured bovine serum albumin (−). Cells were pre-incubated with diluents or desensitized with 100 nM fMLP and then plated in the presence or absence of 10 nM SRSRYp. Cell adhesion onto LM, CG, FN, and VN was considered as 100%, and adhesion to extracellular matrix proteins in the presence of SRSRYp was calculated relative to that. Data represent the average of three experiments, all performed in duplicate, with S.E. indicated by *error bars*. *B*, 293 cells were pre-incubated with diluents or with 5 μg/ml P1F6 anti-αvβ5 mAb or anti-αv Ab or desensitized with 100 nM fMLP, and then they were treated with 10 nM SRSRYp for 10 min. Assessment of ERK1/2 activity was performed as specified under "Experimental Procedures." *C*, adhesion assays of 293 on plastic-immobilized D1, D2, or D3 uPAR domains. Cells were pre-incubated with diluents (□) or 5 μg/ml P1F6 anti-αvβ5 mAb (■) or desensitized with 100 nM fMLP (▨) and then plated in the presence or absence of 10 nM SRSRYp. Cell adhesion onto D1, D2, or D3 uPAR domains was considered as 100%, and cell adhesion in the presence of SRSRYp was calculated relative to that. Data represent the average of three experiments, all performed in duplicate, with S.E. indicated by *error bars*. *D*, 293/uPAR cells treated for 30 min at 37 °C with or without 100 nM fMLP were exposed to the indicated concentrations of SRSRYp for 1 h at 23 °C. 400 μg cell lysate/sample were immunoprecipitated with 5 μg/ml VNR147 anti-αv mAb and loaded onto a 10% SDS-PAGE. 50 μg of 293/uPAR total cell extract or 1 μg of anti-αv mAb was loaded as control. Transferred proteins were revealed with 2 μg/ml R4 anti-uPAR mAb or polyclonal anti-αv Ab.

integrins, binding assays performed by using different plastic-immobilized uPAR domains and cells transfected with different integrins suggest the presence of multiple integrin-binding sites in the uPA receptor (31). With regard to the factors triggering uPAR·integrin association, uPAR engagement by uPA is certainly one of them (8). However, in the uPA-independent model system approached in this study, we found that exogenous SRSRYp is sufficient to increase the uPAR·αvβ5 physical association on the cell membrane. This result is not obvious in view of the fact that SRSRY is not a recognition motif for integrins. Because this effect is abolished by cell desensitization with 100 nM fMLP, a likely possibility is that αvβ5 activation may occur through an FPR-mediated, inside-out type of mechanism. It is possible that the chemotactic uPAR sequence first interacts with FPR, which, in turn, recruits several mediators and affects the activation state of integrins, initiating a signaling cascade. In this model, SRSRY interacts with the fMLP high affinity receptor, which, in turn, changes the αvβ5 activity state, thereby inducing vitronectin release and an increase in uPAR·integrin association. Accordingly, SRSRY triggers FPR signaling by activating both PKC and αvβ5 integrin, the latter of which leads to ERK1/2 phosphorylation. SRSRYp mimics the conformational changes that take place when uPAR is engaged by uPA, leading to receptor cleavage and exposure of the chemotactic sequence. This is also in keeping with the ability of recombinant $D2D3_{88-274}$ to regulate β2 integrin function in monocytes (37). Of course, these observations do not exclude the possibility that different uPAR·αvβ5 contact regions may exist and play specific roles, perhaps in stabilizing pre-existing interactions. In this respect, the relocation of uPAR and its subsequent association with integrins may be influenced also by other forces, such as rafts-directed lateral mobility of glycophosphatidylinositol-anchored proteins. Ligand-dependent interactions may be also important because it has been observed in several cell lines that serine-phosphorylated uPA, which is unable to drive cell migration, also fails to increase the extent of uPAR·integrin association or cause uPAR clustering (38, 39).

TABLE IV
PKC involvement in the SRSRY peptide signaling

293 cells (5×10^4 cells/sample) were incubated with or without 5 μg/ml anti-αvβ5 mAb or anti-αv Ab for 45 min at 23 °C or desensitized with 100 nM fMLP for 30 min at 37 °C. Then, cells were exposed for 5 or 10 min to 10 nM SRSRYp at 23 °C and rapidly lysed. PKC activity was detected by using a protein kinase kit assay. Reaction was allowed to occur for 15 min at 37 °C. PKC activity was determined as pmol phosphate transferred/min. Results were expressed as a mean of values obtained for two experiments, each performed in duplicate.

Pre-treatment	Treatment	PKC activity
None	None	10.9 ± 0.05
None	SRSRY, 5 min	38.0 ± 4
None	SRSRY, 10 min	23.0 ± 6
100 nM fMLP	None	14.2 ± 0.1
100 nM fMLP	SRSRY, 5 min	12.2 ± 0.5
αvβ5 mAb	None	9.2 ± 1.65
αvβ5 mAb	SRSRY, 5 min	38.1 ± 5
αv Ab	None	10.3 ± 0.4
αv Ab	SRSRY, 5 min	40.0 ± 5

The analysis of SRSRY-dependent cell responses sheds light on events that may occur *in vivo* because cleaved forms of uPAR lacking the uPA-binding domain are found in human plasma and urine (23), in blast cells of patients with acute leukemia (40), and in various types of solid tumors (22, 23). Elevated levels of serum uPAR are strongly associated with poor prognosis in tumors (5). Our data suggest that *in vivo* uPAR fragments resulting from receptor shedding and degradation may expose the SRSRY sequence and promote cross-talk between G protein-coupled receptors and integrins. Therefore, it is tempting to speculate that therapeutic targeting of this sequence might interfere with tumor cell migration and invasion.

Acknowledgments—We are grateful to L. Luzzatto for critical review of the manuscript. The technical assistance of A. Arbucci is gratefully acknowledged.

REFERENCES

1. Blasi, F., and Carmeliet, P. (2002) *Nat. Rev. Mol. Biol.* **13,** 932–943
2. Cunningham, O., Andolfo, A., Santovito, M. L., Iuzzolino, L., Blasi, F., and Sidenius, N. (2003) *EMBO J.* **22,** 5994–6003
3. Andreasen, P. A., Kjoller, L., Christensen, L., and Duffy, M. J. (1997) *Int. J. Cancer* **72,** 1–22
4. Dano, K., Romer, J., Nielsen, B. S., Bjorn, S., Pyke, C., Rygaard, J., and Lund, L. R. (1999) *APMIS* **107,** 120–127
5. Sidenius, N., and Blasi, F. (2003) *Cancer Metastasis Rev.* **22,** 205–222
6. Irigoyen, J. P., Munoz-Canoves, P., Montero, L., Koziczak, M., and Nagamine, Y. (1999) *Cell. Mol. Life Sci.* **56,** 104–132
7. Aguirre-Ghiso, J. A., Estrada, Y., Liu, D., and Ossowski, L. (2003) *Cancer Res.* **63,** 1684–1695
8. Carriero, M. V., Del Vecchio, S., Capozzoli, M., Franco, P., Fontana, L., Zannetti, A., Botti, G., D'Aiuto, G., Salvatore, M., and Stoppelli, M. P. (1999) *Cancer Res.* **59,** 5307–5314

9. Chiaradonna, F., Fontana, L., Iavarone, C., Carriero, M. V., Sholz, G., Barone, M. V., and Stoppelli, M. P. (1999) *EMBO J.* **18,** 3013–3023
10. Simon, D. I., Wei, Y., Zhang, L., Rao, N. K., Xu, H., Chen, Z., Liu, Q., Rosenberg, S., and Chapman, H. A. (2000) *J. Biol. Chem.* **275,** 10228–10234
11. Ossowski, L., and Aguirre-Ghiso, J. A. (2000) *Curr. Opin. Cell Biol.* **12,** 613–620
12. Degryse, B., Orlando, S., Resnati, M., Rabbani, S. A., and Blasi, F. (2001) *Oncogene* **20,** 2032–2043
13. Zhang, F., Tom, C. C., Kugler, M. C., Ching, T. T., Kreidberg, J. A., Wei, Y., and Chapman, H. A. (2003) *J. Cell Biol.* **163,** 177–188
14. Wei, Y., Eble, J. A., Wang, Z., Kreidberg, J. A., and Chapman, H. A. (2001) *Mol. Biol. Cell* **12,** 2975–2986
15. Wilcox-Adelman, S. A., Wilkins-Port, C. E., and McKeown-Longo, P. J. (2000) *Cell Adhes. Commun.* **7,** 477–490
16. Sidenius, N., and Blasi, F. (2000) *FEBS Lett.* **470,** 40–46
17. Sidenius, N., Andolfo, A., Fesce, R., and Blasi, F. (2002) *J. Biol. Chem.* **277,** 27982–27990
18. Carriero, M. V., Del Vecchio, S., Franco, P., Potena, M., Chiaradonna, F., Botti, G., Stoppelli, M. P., and Salvatore, M. (1997) *Clin. Cancer Res.* **3,** 1299–1308
19. Kjoller, L., and Hall, A. (2001) *J. Cell Biol.* **152,** 1145–1157
20. Ploug, M. (2003) *Curr. Pharm. Des.* **9,** 1499–1528
21. Hoyer-Hansen, G., Pessara, U., Holm, A., Pass, J., Weidle, U., Dano, K., and Behrendt, N. (2001) *Biochem. J.* **358,** 673–679
22. Sier, C. F., Sidenius, N., Mariani, A., Aletti, G., Agape, V., Ferrari, A., Casetta, G., Stephens, R. W., Brunner, N., and Blasi, F. (1999) *Lab. Investig.* **79,** 717–722
23. Sidenius, N., Sier, C. F., and Blasi, F. (2000) *FEBS Lett.* **475,** 52–56
24. Fazioli, F., Resnati, M., Sidenius, N., Higashimoto, Y., Appella, E., and Blasi, F. (1997) *EMBO J.* **16,** 7279–7286
25. Andolfo, A., English, W. R., Resnati, M., Murphy, G., Blasi, F., and Sidenius, N. (2002) *Thromb. Haemostasis* **88,** 298–306
26. Resnati, M., Pallavicini, I., Wang, J. M., Oppenheim, J., Serhan, C. N., Romano, M., and Blasi, F. (2002) *Proc. Natl. Acad. Sci. U. S. A.* **99,** 1359–1364
27. Montuori, N., Carriero, M. V., Salzano, S., Rossi, G., and Ragno, P. (2002) *J. Biol. Chem.* **277,** 46932–46939
28. Stewart, J. M., and Young, J. D. (1984) in *Solid Phase Peptide Synthesis*, Pierce Chemical, Rockford, IL
29. Del Vecchio, S., Stoppelli, M. P., Carriero, M. V., Fonti, R., Massa, O., Li, P. Y., Botti, G., Cerra, M., D'Aiuto, G., Esposito, G., and Salvatore, M. (1993) *Cancer Res.* **53,** 3198–3206
30. Kusch, A., Tkachuk, S., Haller, H., Dietz, R., Gulba, D. C., Lipp, M., and Dumler, I. (2000) *J. Biol. Chem.* **275,** 39466–39473
31. Tarui, T., Mazar, A. P., Cines, D. B., and Takada, Y. (2001) *J. Biol. Chem.* **276,** 3983–3990
32. Bae, Y. S., Song, J. Y., Kim, Y., He, R., Ye, R. D., Kwak, J. Y., Suh, P. G., and Ryu, S. H. (2003) *Mol. Pharmacol.* **64,** 841–847
33. Kutsuna, H., Suzuki, K., Kamata, N., Kato, T., Hato, F., Mizuno, K., Kobayashi, H., Ishii, M., and Kitagawa, S. (2004) *Am. J. Physiol. Cell Physiol.* **286,** C55–C64
34. Spisani, S., Falzarano, S., Traniello, S., Nalli, M., and Selvatici, R. (2005) *FEBS J.* **272,** 883–891
35. Gellert, G. C., Goldfarb, R. H., and Kitson, R. P. (2004) *Biochem. Biophys. Res. Commun.* **315,** 1025–1032
36. Aguirre-Ghiso, J. A., Liu, D., Mignatti, A., Kovalski, K., and Ossowski, L. (2001) *Mol. Biol. Cell* **12,** 863–879
37. Furlan, F., Orlando, S., Laudanna, C., Resnati, M., Basso, V., Blasi, F., and Mondino, A. (2004) *J. Cell Sci.* **117,** 2909–2916
38. Franco, P., Iaccarino, C., Chiaradonna, F., Brandazza, A., Iavarone, C., Mastronicola, M. R., Nolli, M. L., and Stoppelli, M. P. (1997) *J. Cell Biol.* **137,** 779–791
39. Carriero, M. V., Franco, P., Gargiulo, L., Vocca, I., Cito, L., Fontana, L., Iaccarino, C., Del Pozzo, G., Guardiola, J., and Stoppelli, M. P. (2002) *Biol. Chem.* **383,** 107–113
40. Mustjoki, S., Sidenius, N., Sier, C. F., Blasi, F., Elonen, E., Alitalo, R., and Vaheri, A. (2000) *Cancer Res.* **60,** 7126–7132

Cross-talk between fMLP and Vitronectin Receptors Triggered by Urokinase Receptor-derived *SRSRY* Peptide

Lucia Gargiulo, Immacolata Longanesi-Cattani, Katia Bifulco, Paola Franco, Rosanna Raiola, Pietro Campiglia, Paolo Grieco, Gianfranco Peluso, M. Patrizia Stoppelli and Maria V. Carriero

J. Biol. Chem. 2005, 280:25225-25232.
doi: 10.1074/jbc.M412605200 originally published online May 2, 2005
